Available online at www.sciencedirect.com

SciVerse ScienceDirect

Energy Procedia 37 (2013) 331 – 339

Energy Procedia

GHGT-11

Selection and characterization of phase-change solvent for carbon dioxide capture: precipitating system

Sholeh Ma'mun*, Inna Kim

SINTEF Materials and Chemistry, N-7465 Trondheim, Norway

Abstract

Characterization of a precipitating solvent for CO_2 capture was performed. Aqueous solution of 5m' potassium salt of sarcosine (KSar) that was precipitated at CO_2 loading of 0.52 was selected. The equilibrium solubility of CO_2 in the solution was measured over a range of temperatures from 40 to 120 °C. The SOFT model was implemented to predict the vapor-liquid-solid equilibrium (VLSE) data for the CO_2-KSar-H_2O system. The vapor pressures of the solution were measured at temperatures between 53 and 130 °C. The heat of absorption was also measured at 40 °C. In addition, the heat of absorption of CO_2 in the solution was estimated from the VLSE data by use of the Gibbs-Helmholtz equation and was able to predict well the precipitation occurred in the system.

Selection and/or peer-review under responsibility of GHGT

Keywords: carbon dioxide capture; absorption; equilibrium; amino acid salt; precipitating system

1. Introduction

Carbon dioxide (CO_2) is produced in large quantities from industrial processes, such as steel and cement production, coal-fired power plants, petrochemical manufacturing, and natural gas processing. Thus, intensive research on CO_2 Capture and Sequestration (CCS) is being conducted to mitigate CO_2 emission which is found to be a major contributor for the global climate change facing the world community.

Absorption process using amine-based solvents (MEA- and AMP-based) is the lead contending technology today. This process is found to be the most practicable given the state of current knowledge [1]. An economic study also indicates that the process will also remain competitive in the future [2]. One of the key improvements under solvent development is to find new, faster, and more energy-efficient

* Corresponding author. Tel.: +47-98283950; fax: +47-73593000.
E-mail address: Sholeh.Mamun@sintef.no

1876-6102
Selection and/or peer-review under responsibility of GHGT
doi:10.1016/j.egypro.2013.05.119

absorbents [3]. Therefore, research has focused on meeting this goal by testing alternative alkanolamines and their blends, sodium carbonate solutions, chilled ammonia, and amino acid salts [4−13].

The amino acid salts were traditionally used in the acid gas removal as promoters for the conventional gas treating solvents, such as glycine, alanine and diethyl or dimethyl glycine [14]. A range of absorption liquids based on amino acid salts so-called "CORAL" was developed and patented by TNO [11].

Formation of a solid phase due to precipitation during absorption of CO_2 with aqueous solutions can be found in the systems such as chilled ammonia, carbonates, concentrated piperazine, and amino acid salts. Normally, precipitation is avoided in the CO_2 capture processes. However, if the precipitant contains CO_2 (i.e., carbamate, carbonate/bicarbonate), the driving force may be maintained at increased loading, so that higher solvent loadings may be reached resulting in lower energy consumption for the solvent regeneration [15]. If the precipitant is an acid compound, precipitation in the absorber induces a shift to a higher pH at which higher CO_2 loadings (α_{CO2}) can be achieved. At the same time, precipitation usually happens at high CO_2 loadings and if the precipitate is an amine base, the reaction equilibrium is shifted enhancing the release of CO_2, thus giving new possibilities for the stripping. However, experimental data proving these claims are very limited in the literature. The only systematic study on precipitation at process conditions and evaluation of the concept was done for the Alstom Chilled Ammonia Process [9].

In this work, a potassium amino acid salt, i.e., potassium salt of sarcosine (KSar), was selected for further study based on a comparative screening experiment by Aronu et al. [16]. It was found that KSar gives high rate of absorption and high loading capacity in comparison to MEA. In addition, KSar shows slightly different behavior during CO_2 absorption. At high CO_2 loadings, an increase in the absorption rate was observed for this system when precipitation starts to occur. In-situ monitoring of precipitation can be performed by use of Focused Beam Reflectance Measurement (FBRM) and Particle Vision and Measurement (PVM). In addition, vapor-liquid-solid equilibria (VLSE) and heat of absorption were also measured.

2. Materials and methods

2.1. Materials

The CO_2 (99.999 vol%) and N_2 (99.999 vol%) gases were obtained from Yara-Praxair. Monoethanolamine [MEA, $H_2N(CH_2)_2OH$] was obtained from Sigma-Aldrich with purity of min. 99% and was used without further purification. Sarcosine (CH_3NHCH_2COOH) and potassium hydroxide (KOH) were obtained from Sigma-Aldrich and Merck Chemicals with purities of min. 98% and min. 85%, respectively. Potassium salt of sarcosine (KSar) with concentration of 5 m' (mol/kg-solution) was prepared by neutralizing 5 moles of sarcosine with an equimolar amount of KOH in a total solution weight of 1 kg.

2.2. Vapor pressure and VLSE measurements

Vapor pressure measurement of the aqueous solution of KSar was performed in a modified Swietoslawski ebulliometer. The scheme of the experimental set-up and the operating procedure can be found in Kim et al. [17]. For the VLSE measurement at low temperatures up to 80 °C, a commercially available automatic laboratory reactor Mettler Toledo LabMax® as shown in Figure 1 was used. The apparatus consists of a 1−L mechanically agitated-jacketed glass reactor equipped with temperature, pressure, and pH-probes. This set-up is also equipped with an external thermocouple, two RMS multimeters, a Bühler gas pump, a Rosemount BINOS 100 IR CO_2 analyzer, and a Bronkhorst® Hi-Tec N_2/CO_2 mass flow controller. For in-situ monitoring of precipitation, two probes are installed:

- FBRM gives information on particles size (chord length) distribution. Start of precipitation (formation of the crystals) as well as complete dissolution (disappearance of the crystals) may be clearly seen on the FBRM curves.
- PVM provides in-situ images to characterize particles from 2 μm to 1 mm size in concentrations up to 40% solids and higher.

Before starting the experiment, the IR analyzer was calibrated using CO_2/N_2 gas mixture with different compositions. Unloaded KSar solution of 600 mL was fed into the rector. Carbon dioxide was added by bubbling it into the solution to obtain a certain CO_2 loading. The reactor was heated at a desired temperature with a constant heat rate of 3 °C/min. The gas pump circulates the gas phase from the rector through the CO_2 analyzer and back to the reactor through the liquid phase. The equilibrium was obtained when the analyzer showed a constant value for the CO_2 volume percent. This took about 1 – 2 hrs.

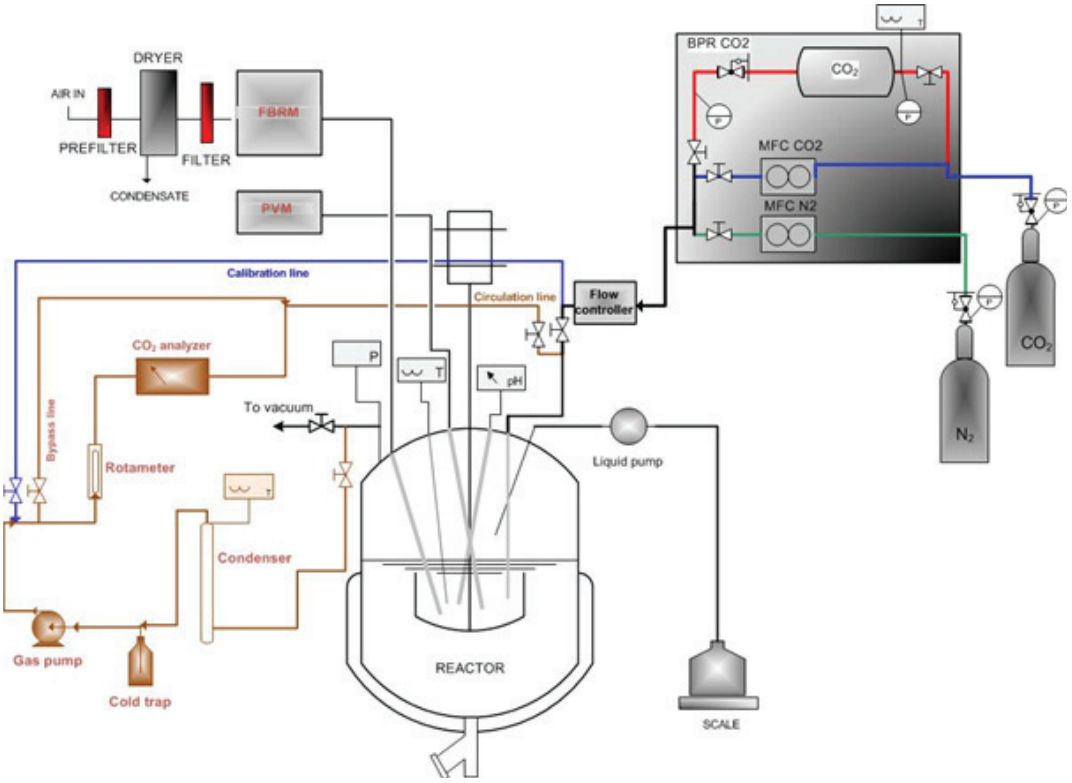

Figure 1. Experimental set-up for VLSE measurements and crystallization study

A liquid sample of 10 mL to be analyzed for CO_2 and total alkalinity concentrations was then withdrawn from the reactor. The CO_2 concentration was measured by a GC Apollo 9000 Combustion TOC Analyzer and by the precipitation-titration method as described in Ma'mun et al. [3], whereas the total alkalinity concentration was determined by an automatic titrator Metrohm 905 Titrando.

The gas bleed extracted for composition measurement was cooled to about 15 °C to condense the gas phase and the CO_2 content was directly determined by the IR analyzer. The concentration of CO_2 in the analyzer is calculated by the Eq. (1).

$$y_{CO_2}^{IR} = \frac{n_{CO_2}^{IR}}{n_{CO_2}^{IR} + n_{N_2}^{IR} + n_{H_2O}^{IR} + n_{Solvent}^{IR}} \quad (1)$$

where *n* denotes molar flow and the superscript IR denotes the gas phase in the IR analyzer. If vapor pressure data of the solution are available, the partial pressure of CO_2 can then be calculated as

$$p_{CO_2} = y_{CO_2}^{IR}\left[P - \left(p_{Solution} - p_{Solution}^{IR}\right)\right] \quad (2)$$

The VLSE measurement at high temperatures up to 120 °C was conducted in a rocking unit apparatus. The experimental set-up and the operating procedure can be found in Ma'mun et al. [18].

At higher CO_2 loadings, the solution may start to precipitate and start to form crystals. The growth of crystals increases as CO_2 loading increases. During this period, PVM can be used to observe the growth of crystals by taking their images.

2.3. Heat of absorption measurement

The reaction calorimeter used to measure the heat of absorption of CO_2 in 5m' KSar solution was a 2−L mechanically agitated reactor. The reaction vessel is suitable for work under pressures up to 100 barg and at temperatures up to 200 °C. The system provides a measure of the heat flow in real time. The scheme of the experimental set-up and its operating procedure was explained in detail by Kim and Svendsen [19].

3. Results and discussion

3.1. Validation of LabMax® set-up for VLE measurement

In addition to studying crystallization process, the LabMax® set-up is also capable of measuring vapor-liquid equilibria (VLE) by installing additional instruments such as IR analyzer, gas pump, and cooler. To meet the goal, a validation of the set-up for the VLE measurement by a known system needs to be conducted. This was performed by measuring the solubility of CO_2 in 30 mass % MEA solution. The VLE validation results are depicted in Figure 2. It is clear from the Figure that the results in this work are found to be in a good agreement with the data from Jou et al. [20] and those from Aronu et al. [21] at temperatures from 40 to 80 °C. Based on these VLE validation results, the LabMax® set-up can, therefore, serve as an alternative to the existing VLE apparatuses. In addition, the set-up offers some advantages in comparison to the low temperature VLE set-up previously used by Ma'mun et al. [3] and Aronu et al. [21]. There is no need to preload the solution with CO_2 before feeding it into the reactor. This is done by adding CO_2 directly to the reactor at a desired CO_2 loading. The reactor is also equipped by a stirrer, thus the equilibrium can be achieved faster.

The partial pressures of CO_2 were calculated by use of Eq. (2) in which the vapor pressures of the solution were obtained from the experiment by use of the ebulliometer. Figure 2a shows the experimental vapor pressure data for both 30 mass % MEA and 5m' KSar solutions together with their fitting data by means of Antoine equations. It can be seen from the Figure that KSar solution is less volatile than MEA which leads to less solvent make-up in the absorption process. This shows one of the advantages of the amino acid systems for the CO_2 capture processes.

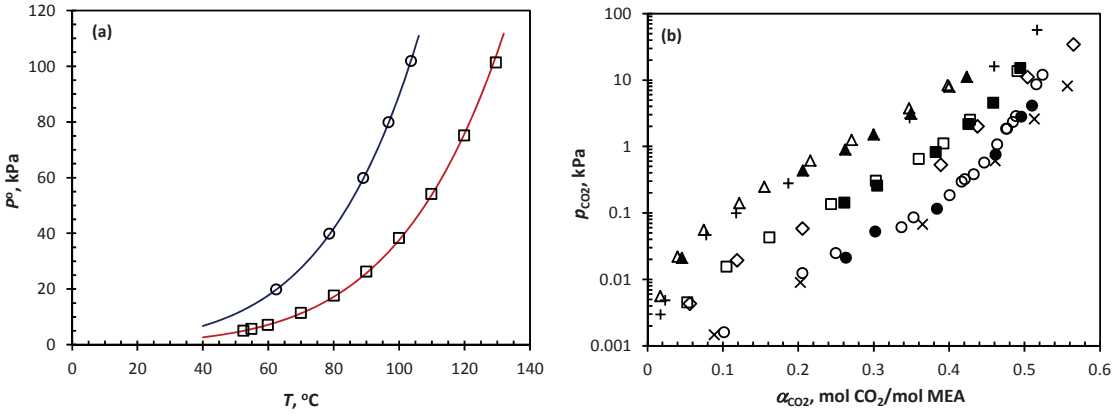

Figure 2. (a) Vapor pressure of solutions: ○, 30 mass % MEA; □, 5m' KSar; lines were calculated by the Antoine equation. (b) Equilibrium solubility of CO_2 in 30 mass % MEA solution using LabMax® set-up at 40, 60 and 80 °C. This work: ●, 40 °C; ■, 60 °C; ▲, 80 °C; Jou et al. [20]: ×, 40 °C; ◊, 60 °C; +, 80 °C; Aronu et al. [21]: ○, 40 °C; □, 60 °C; Δ, 80 °C.

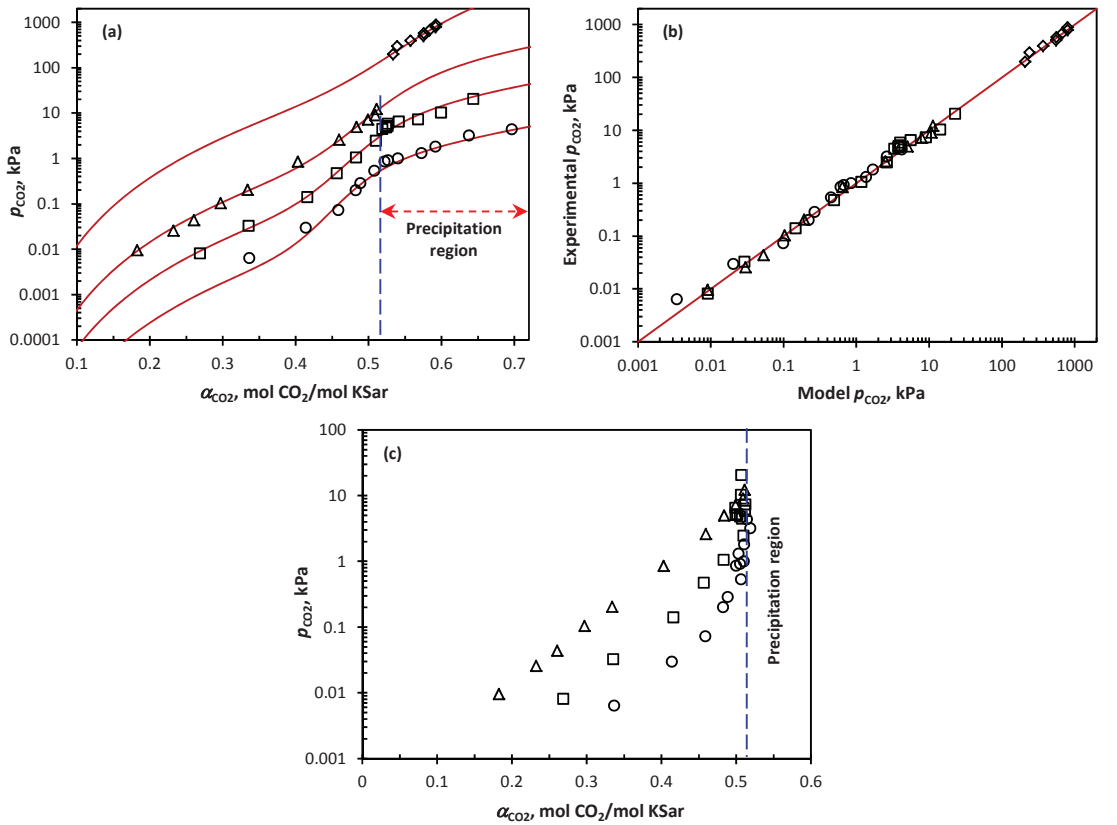

Figure 3. Equilibrium solubility of CO_2 in 5m' KSar solution. All data points were measured in this work: ○, 40 °C; □, 60 °C; Δ, 80 °C; ◊, 120 °C. (a) Curves were calculated by the SOFT model at different temperatures. (b) Parity plot between the experimental CO_2 partial pressures and those calculated from the model. (c) Liquid-phase analysis results.

3.2. Vapor-liquid-solid equilibria and SOFT modeling

The VLSE measurement of the CO_2 solubility in 5m' KSar solution was conducted over a range of temperatures from 40 to 120 °C. In addition, a SOFT modeling approach was used to predict the VLSE data. SOFT system is a type of equilibrium model used for systems with limited available data. The model gives equilibrium partial pressure of CO_2 over a solvent system based on a functional fitting towards experimental data as function of liquid CO_2 loading and temperature. In this type of model, no activity coefficients are needed nor calculated. Figure 3a shows the experimental VLSE data together with the SOFT model calculation results at different temperatures. It is clearly seen from Figure 3a that the SOFT model gives a good representation of the experimental data used in the regression analysis. The average absolute relative deviation (AARD) between the experimental CO_2 partial pressures and those calculated from the model is 14.7%. The Figure also shows that both slopes of the equilibrium curves at 40 and 60 °C decrease (i.e., less steep) in the precipitation region. As a consequence, this condition will keep the driving force high (i.e., CO_2 absorption rate remains high), thereby increasing the solvent capacity. This is also one of the advantages of the precipitating system for the CO_2 capture processes. The parity plot of the experimental CO_2 partial pressures and those from the model is depicted in Figure 3b. It can be seen from the Figure that the experimental data points are well distributed by the model.

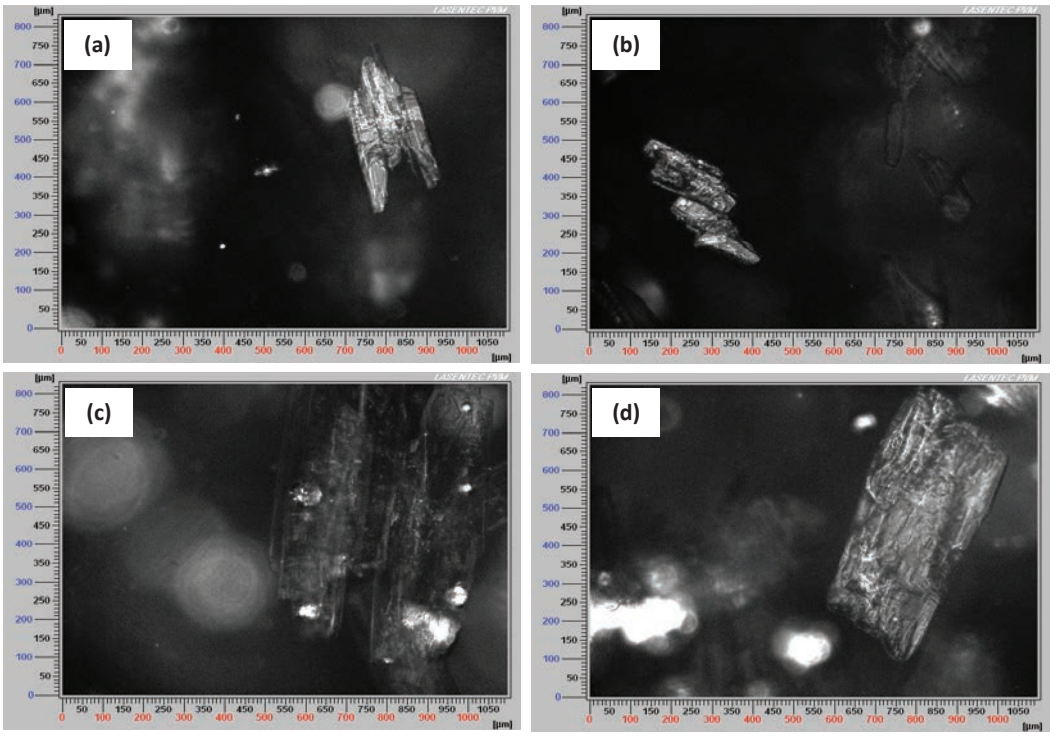

Figure 4. The crystal images taken by PVM. (a) 40 °C, α_{CO2} = 0.54; (b) 60 °C, α_{CO2} = 0.54; (c) 40 °C, α_{CO2} = 0.64; (d) 60 °C, α_{CO2} = 0.64.

It was clearly observed that precipitation occurred in the system at CO_2 loadings higher that 0.52 at 40, 60 and 80 °C. The precipitation was not able to observe at 120 °C due to using another type of set-up (i.e., a stainless rector). During the 120 °C sampling, a certain amount of fresh solution was also added into the

sampling cylinder to dilute the sample taken from the reactor. Moreover, to confirm that the precipitation has started to occur at the CO_2 loading of 0.52, all the precipitated liquid samples at 40, 60 and 80 °C were analyzed for the liquid phase. The results show that the liquid phase of the precipitated samples gave the similar CO_2 loading of 0.52 as depicted in Figure 3c.

In this work, some crystal images were also taken by use of PVM at different CO_2 loadings and at different temperatures. Figure 4 shows the images at 40 and 60 °C and at CO_2 loadings of 0.54 and 0.64, respectively. It can be seen from the Figure that the crystal size increases as the CO_2 loading increases at the same temperature.

Based on the VLSE data at absorption and desorption temperatures, 40 and 120 °C respectively, a net cyclic capacity (i.e., in mole of CO_2 absorbed per kg of solution) of 5m' KSar solution can be determined, so that its net cyclic capacity can then be compared to that of 30 mass % MEA solution. A method to determine the net cyclic capacity can be found in Ma'mun et al. [4]. In this method, it is assumed that equilibrium is attained in both the absorption and stripping steps. As an example, at CO_2 partial pressure of 10 kPa, MEA will give lean and rich loadings of 0.18 and 0.52 respectively, thereby giving a net cyclic capacity of 1.67 mol CO_2 / kg solution. At the same CO_2 partial pressure, the lean and the rich loadings of KSar are 0.38 and 0.83, respectively, giving the net cyclic capacity of 2.23 mol CO_2 / kg solution which is 34% higher than the net cyclic capacity of MEA. This is another important benefit given by KSar in comparison to MEA.

3.3. Heat of absorption

A method to measure the heat of absorption of CO_2, ΔH_{abs}, in an absorbent, i.e., differential in temperature and semi-differential in loading, has been proposed by Kim and Svendsen [19]. In this work, the differential of ΔH_{abs} in aqueous solutions of 3.5m' and 5m' KSar was measured over the temperature range from 40 to 120 °C. As seen in Figure 5a, there is a difference pattern of the ΔH_{abs} between in 3m' and 5m' KSar solutions, for instance. The ΔH_{abs} in both concentrations gives almost similar values at the CO_2 loadings lower than 0.35. At the CO_2 loadings higher than 0.35, the ΔH_{abs} in 3.5m' KSar solution decreases as the loading increases, while that in 5m' KSar solution starts to decrease at the loading of 0.43 and reaches the minimum value at the loading of 0.52. At this loading point, the solution starts to precipitate and, as a result, the ΔH_{abs} starts to increase again and then decreases smoothly as the loading increases.

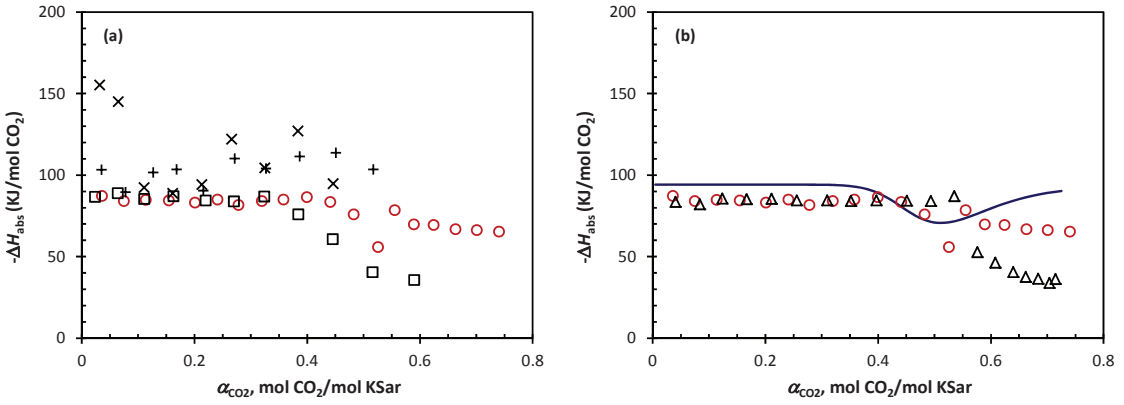

Figure 5. (a) Heat of absorption of CO_2 in two different concentrations of KSar solutions: □, 40 °C; +, 80 °C; ×, 120 °C (3.5m' KSar); ○, 40 °C (5m' KSar). (b) Comparison of heat of absorption at 40 °C: ○, 5m' KSar; Δ, 30 mass % MEA [19]. Solid line was calculated by the Gibbs-Helmholtz equation from the VLSE data of 5m' KSar solution.

A comparison of the ΔH_{abs} of CO_2 in KSar and MEA solutions at 40 °C is depicted in Figure 5b. It can be seen from the Figure that the ΔH_{abs} in 5m' KSar solution has similar values with that in 30 mass % MEA solution published by Kim and Svendsen [19] at the loadings lower than 0.45, but gives higher values at the loading higher than 0.56. The ΔH_{abs} in KSar solution is, therefore, somewhat slightly higher than that in MEA solution at 40 °C.

Figure 5b also shows an estimation of the ΔH_{abs} calculated from the VLSE model of the CO_2 solubility in the 5m' KSar solution by use of the Gibbs-Helmholtz equation as follows:

$$\left(\frac{\partial \ln p_{CO_2}}{\partial (1/T)}\right)_{\alpha_{CO_2}} = \frac{-\Delta H_{abs}}{R} \tag{3}$$

where α_{CO2} is the CO_2 loading. The ΔH_{abs} estimated by the Gibbs-Helmholtz equation is an aggregate form of them over a certain temperature range and dependent on the CO_2 loading. The method does not necessarily, according to Kim and Svendsen [19], give an accurate description of the ΔH_{abs} values. As mentioned above, the 5m' KSar and 30 mass % MEA systems give, respectively, the lean loadings of 0.18 and 0.38 at the same CO_2 partial pressure of 10 kPa. At this condition, both systems give similar values of the ΔH_{abs}, which is found be 90 kJ/mol CO_2, as reported by Aronu et al. [21] for 30 mass % MEA. It can also be seen in the Figure, the estimated ΔH_{abs} by use of the Gibbs-Helmholtz equation is able to well predict where the precipitation starts. This occurs at the CO_2 loading of 0.52 where the ΔH_{abs} reaches the minimum value.

4. Conclusion

The aqueous solution of 5m' potassium salt of sarcosine (KSar) was selected based on a solvent screening study and was further characterized. In this work, some measurements were conducted, such as vapor pressure, vapor-liquid-solid equilibrium and heat of absorption measurements. The experimental results show that KSar solution has a better performance in comparison to that of MEA in which KSar system gives lower vapor pressure and also offers higher net cyclic capacity. The heat of absorption of CO_2 in KSar solution is relatively the same as that in 30 mass % MEA at 40 °C. The estimated heat of absorption by use of the Gibbs-Helmholtz equation is also able to predict the start of precipitation. In addition, the experimental VLSE data can well be represented by the SOFT model implemented in this KSar system.

Acknowledgements

This publication is produced with support from the BIGCCS Centre, performed under the Norwegian research program *Centres for Environment-friendly Energy Research (FME)*. The authors acknowledge the following partners for their contributions: Aker Solutions, ConocoPhilips, Det Norske Veritas AS, Gassco AS, GDF SUEZ, Hydro Aluminium AS, Shell Technology AS, Statkraft Development AS, Statoil Petroleum AS, TOTAL E&P Norge AS, and the Research Council of Norway (193816/S60).

References

[1] Meisen A, Shuai X. Research and development issues in CO_2 capture. *Energ Convers Manage* 1997; **38**: Suppl., S37−S42.

[2] Desideri U, Corbelli R. CO_2 capture in small size cogeneration plants: technical and economical considerations. *Energ Convers Manage* 1998, **39**: 857–67.

[3] Ma'mun S, Jakobsen JP, Svendsen HF, Juliussen O. Experimental and modeling study of the solubility of carbon dioxide in aqueous 30 mass % 2-((2-aminoethyl)amino)ethanol solution. *Ind Eng Chem Res* 2006; **45**: 2505−12.

[4] Ma'mun S, Svendsen HF, Hoff KA, Juliussen O. Selection of new absorbents for carbon dioxide capture. *Energ Convers Manage* 2006; **48**: 251−8.

[5] Singh P, Niederer J, Versteeg G. Structure and activity relationships for amine based CO_2 absorbents – I. *Int J Greenh Gas Con* 2007; **1**: 5−10.

[6] Idem R, Wilson M, Tontiwachwuthikul P, Chakma A, Veawab A, Aroonwilas A, Gelowitz D. Pilot plant studies of the CO_2 capture performance of aqueous MEA and mixed MEA/MDEA solvents at the University of Regina capture technology development plant and the Boundary Dam CO_2 capture demonstration plant. *Ind Eng Chem Res* 2006; **45**: 2414−20.

[7] Cullinane JT, Rochelle GT. Carbon dioxide absorption with aqueous potassium carbonate promoted by piperazine. *Chem Eng Sci* 2004; **59**: 3619−30.

[8] Lu Y, Ye X, Zhang Z, Khodayari A, Djukadi T. Development of a carbonate absorption-based process for post-combustion CO_2 capture: The role of biocatalyst to promote CO_2 absorption rate. *Energy Procedia* 2011; **4**: 1286−93.

[9] Alstom. Chilled ammonia-based wet scrubbing for post-combustion CO_2 capture. DOE/NETL report 2007; No. 401/021507.

[10] Chen H, Dou B, Song Y, Xu Y, Wang X, Zhang Y, Du X, Wang C, Zhang X, Tan C. Studies on absorption and regeneration for CO_2 capture by aqueous ammonia. *Int J Greenh Gas Con* 2012; **6**: 171−8.

[11] Kumar PS, Hogendoorn JA, Feron PHM, Versteeg GF. New absorption liquids for the removal of CO_2 from dilute gas streams using membrane contactors. *Chem Eng Sci* 2002; **57**: 1639−51.

[12] Jockenhövel T, Schneider R. Towards commercial application of a second-generation post-combustion capture technology – Pilot plant validation of the Siemens capture process and implementation of a first demonstration case. *Energy Procedia* 2011; **4**: 1451−58.

[13] Knuutila H, Aronu UE, Kvamsdal HM, Chikukwa A. Post combustion CO_2 capture with an amino acid salt. *Energy Procedia* 2001; **4**: 1550−57.

[14] Kohl A L, Nielsen R. *Gas purification.* 5th ed. Houston: Gulf Publishing Company; 1997.

[15] Feron PHM, ten Asbroek N. *New solvents based on amino-acid salts for CO_2 capture from flue gases*. GHGT-7, Vancouver, Canada; 2004.

[16] Aronu UE, Ciftja AF, Kim I, Hartono A. *Understanding precipitation in amino acid salt systems at process conditions.* Submitted to GHGT-11, Kyoto, Japan; 2012.

[17] Kim I, Svendsen HF, Børresen E. Ebulliometric determination of vapor-liquid equilibria for pure water, monoethanolamine, N-methyldiethanolamine, 3-(methylamino)-propylamine, and their binary and ternary solutions. *J Chem Eng Data* 2008; **53**: 2521–31.

[18] Ma'mun S, Nilsen R, Svendsen HF. Solubility of carbon dioxide in 30 mass% monoethanolamine and 50 mass% methyldiethanolamine solutions. *J Chem Eng Data* 2005; **50**: 630−4.

[19] Kim I, Svendsen HF. Heat of absorption of carbon dioxide (CO_2) in monoethanolamine (MEA) and 2-(aminoethyl)ethanolamine (AEEA) solutions. *Ind Eng Chem Res* 2007; **46**: 5803−09.

[20] Jou FY, Mather AE, Otto FD. The solubility of CO_2 in a 30 mass percent monoethanolamine solution. *Can J Chem Eng* 1995; **73**: 140−7.

[21] Aronu UE, Gondal S, Hessen ET, Warberg TH, Hartono A, Hoff KA, Svendsen HF. Solubility of CO_2 in 15, 30, 45 and 60 mass % MEA from 40 to 120 °C and model representation using the extended UNIQUAC framework. *Chem Eng Sci* 2011; **66**: 6393–406.